Gap junctions destroy persistent states in excitatory networks

Bard Ermentrout
Department of Mathematics, University of Pittsburgh, Pittsburgh, Pennsylvania 15260, USA
(Received 23 May 2006; published 27 September 2006)

Gap junctions between excitatory neurons are shown to disrupt the persistent state. The asynchronous state of the network loses stability via a Hopf bifurcation and then the active state is destroyed via a homoclinic bifurcation with a stationary state. A partial differential equation (PDE) is developed to analyze the Hopf and the homoclinic bifurcations. The simplified dynamics are compared to a biophysical model where similar behavior is observed. In the low noise case, the dynamics of the PDE is shown to be very complicated and includes possible chaotic behavior. The onset of synchrony is studied by the application of averaging to obtain a simple criterion for destabilization of the asynchronous persistent state.

DOI: 10.1103/PhysRevE.74.031918 PACS number(s): 87.19.La, 05.45.−a, 87.10.+e

I. INTRODUCTION

Persistent activity in populations of coupled neurons is believed to underly many neural phenomena both normal and pathological. For example, persistent activity has been suggested as a mechanism for working memory [1,2] as well as underlying epileptic activity in pharmacologically manipulated tissue [3,4]. The principle theoretical hypothesis for the mechanism of persistent activity is via recurrent synaptic interactions between excitatory neurons. There has recently been a great deal of experimental and theoretical interest in role of gap junction (electrical) coupling in synchronizing populations of inhibitory interneurons [5–9]. Despite the plethora of experimental evidence for electrical coupling between *inhibitory* neurons, there are very few instances showing such coupling between excitatory neurons [10,11]. In this paper, we suggest that the reason for the lack of gap junctions between excitatory neurons is that such junctions could disrupt the ability of networks to form persistent activity. Specifically, gap junctions have a tendency to synchronize neurons and it has been shown that synchrony often destroys persistent activity [12–17]. Indeed, Netoff and Schiff [3] show that the termination of ictal seizure events is presaged by increase in synchrony between neighboring neurons. Hughes *et al.* [11] have suggested that there may be some gap junctional coupling between thalamocortical neurons but these neurons are not known to produce persistent activity. Traub and collaborators have suggested that gap junctions between axons which spontaneously fire action potentials can serve as background activity to engage inhibitory oscillatory networks responsible for gamma rhythms [10]. However, it is not known whether these networks are involved in the kind of persistent activity which underlies working memory or other phenomena described above.

In this paper, we start with some simulations of a conductance based model in which we induce a persistent state via strong recurrent excitatory connections and show how this is destroyed by gap junctions. Then we turn to a simplified scalar model which we reduce to a partial differential equation for the distribution of states (Fokker-Planck equation). We discretize the PDE and use continuation to analyze the mechanism through which gap junctions disrupt the persistent state. We show that there is a Hopf bifurcation corresponding the synchronized spiking of the network. As the gap junctions increase, the magnitude of the mean field synaptic oscillation increases and becomes homoclinic to a stationary distribution of the PDE and then disappears destroying the active state. We return to the conductance based model and derive a formula for the critical gap junction strength leading to synchrony. We then use simulations to show that the full conductance-based model appears to undergo a similar transition via a homoclinic orbit.

II. CONDUCTANCE-BASED MODEL

The conductance-based model consists of 100 globally coupled single compartment neurons each having a leak, a sodium current, and a delayed rectifier current. The model is based on channel kinetics in Refs. [18–20]. Details of the channel kinetics are in Appendix A. The network has the form

$$C\frac{dV_j}{dt} = -g_L(V_j - E_L) - g_K n_j^4 (V_j - E_K) - g_{Na} m_j^3 h_j (V - E_{Na}) \tag{1}$$

$$- g_{\text{gap}}(V_j - \bar{V}) - g_{\text{syn}} \bar{s} V_j + \sigma \xi(t), \tag{2}$$

$$\frac{ds_j}{dt} = 2(1 - s_j)/[1 + \exp(-V_j/4)] - s_j/3, \tag{3}$$

$$\bar{V} = \frac{1}{N}\sum_k V_k,$$

$$\bar{s} = \frac{1}{N}\sum_k s_k,$$

where the channel variables m,h,n satisfy equations of the form

$$\frac{dx}{dt} = a_x(V)(1 - x) - b_x(V)x.$$

Each neuron has independent white noise added to it with zero mean and variance $\sigma^2/2C^2$. Typically, $\sigma=0.1$.

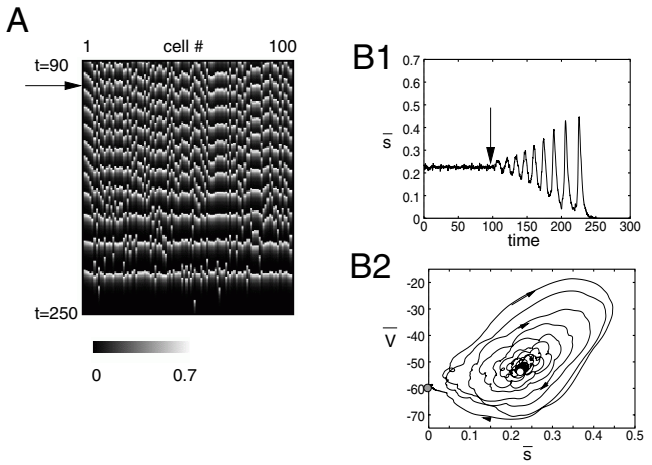

FIG. 1. Persistent activity is disrupted with gap junctions. (A) Synaptic activity $s_j(t)$ for all 100 neurons for $90<t<250$ ms. At $t=100$, the gap junctional coupling is increased from 0 to 0.05, synchronizing the network and destroying the persistent state. (B1) $\bar{s}$ shows the onset of synchrony with increasing amplitude and death. (B2) Same as (B1) but plotted in the phase plane showing $\bar{V}$ as well. White circle is steady state persistent state when there is no gap junctional coupling.

Equations are integrated using Euler's method with a step size of 10 microseconds. We used $N=100$.

A network of conductance-based neurons with all-all excitatory synaptic coupling and a small amount of noise is able to support a persistent asynchronous state if the model cells are sufficiently stimulated. Figure 1 shows an example of this persistent state. Noise is not necessary but enhances the asynchronous behavior. This phenomena is well known and has been studied in both conductance-based models as well as simplified integrate-and-fire systems. In Fig. 1(A), at $t=100$ ms, the gap junctions are turned on. Over the next 150 ms, the neurons appear to synchronize and once synchrony is reached, the persistent state disappears. Figure 1(B1) shows the total synaptic activity as a function of time, $\bar{s}=(1/N)\Sigma s_j$. The persistent state $\bar{s}\approx 0.23$ shows some small fluctuations until $t=100$ when the gap junctions are activated. $\bar{s}$ undergoes growing oscillations and at $t\approx 220$ goes to zero as the neurons return to rest. Figure 1(B2) shows the same transition in the $(\bar{s},\bar{V})$ phase plane. Here $\bar{V}=(1/N)\Sigma V_j$. The persistent state is indicated by the white circle at (0.23, −45). The persistent state terminates at the resting potential of the cell, indicated by the gray circle at (0, −60).

Our goal in this paper is to understand and explain Fig. 1. How is it that electrical coupling destroys the persistent state? On possibility is that electric coupling decreases the resistance of the cell (acts similar to a shunt) and thus renders the synaptic excitation less effective. Another possibility is that the electrical coupling destabilizes the persistent state. The former mechanism is static while the other requires looking at the dynamics. We first show that the shunting hypothesis is incorrect.

Conditions for the persistent state to exist can be found self-consistently by making the ansatz that the neurons all fire asynchronously and that there is no noise. This means that the network average of the synaptic gates, s_j and the voltages, V_j are constant and the same as the time averages of the individual synapse and potential

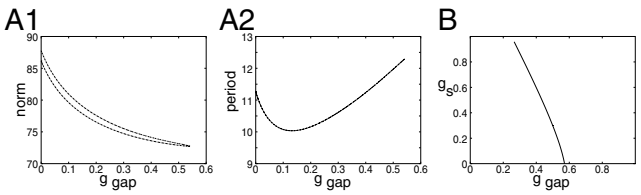

FIG. 2. Existence of the persistent state as the gap junctional coupling increases. (A1) Norm of the solution to the self-consistent boundary value problem as g_{gap} increases when $g_{\text{syn}}=0.15$. At $g_{\text{gap}}\approx 0.55$ the solution with $V(0)=0$ ceases to exist. (A2) The period is a nonmonotonic function of the electrical coupling. (B) Two parameter diagram showing critical electrical coupling strength as the synaptic coupling changes.

$$\bar{s}\equiv \lim_{N\to\infty}\frac{1}{N}\sum_j s_j=\frac{1}{P}\int_0^P s_i(t)dt \quad \forall\, i,$$

$$\bar{V}\equiv \lim_{N\to\infty}\frac{1}{N}\sum_j V_j=\frac{1}{P}\int_0^P V_i(t)dt \quad \forall\, i.$$

Here P is the period of the oscillation of a single neuron. Thus, we need to solve the following differential equation:

$$C\frac{dV}{dt}=-I_{\text{ion}}(V,m,h,n)-g_{\text{syn}}\bar{s}(V-E_{\text{syn}})+g_{\text{gap}}(\bar{V}-V),$$

$$\bar{s}=\frac{1}{P}\int_0^P s(t)dt,$$

$$\bar{V}=\frac{1}{P}\int_0^P V(t)dt$$

along with the dynamics for s,m,h,n which must be periodic. Since periodic solutions are translation invariant, we fix the phase of the oscillation by setting $V(0)=0$. This guarantees that the neuron is actually spiking.

It is easy to numerically solve the ODE self-consistently by treating it as a boundary-value problem (BVP). (See Appendix B for the form of the BVP.) Figure 2(A1) shows the numerical solution for the persistent state as the strength of electrical coupling increases. There is a turning point or fold bifurcation at $g_{\text{gap}}\approx 0.55$ and there appear to be two branches of solutions. One surprising result is that the frequency actually increases for small electric coupling [as shown in Fig. 2(A2)]. Another interesting result is that the critical gap junctional strength actually decreases with stronger synaptic excitation [Fig. 2(B)] even though synaptic coupling is a desynchronizing influence. Clearly the persistent state *exists* for g_{gap} up to 0.55 when $g_{\text{syn}}=0.15$. However, in Fig. 1 we saw that g_{gap} as small as 0.05 was sufficient to destroy the persistent state. Thus, we conclude that while the persistent state exists, it appears to lose stability as the gap

junction strength increases. Shunting is not sufficient to explain the loss of a stable persistent state.

We conclude this part of the analysis with rough estimate of the self-consistent value of $\bar{s}$ when there is no electrical coupling. Such calculations are routine, for example, Refs. [1,12,15]. Consider $\bar{s}$ as a parameter. Then we have to solve the single cell model for $V(t)$. Since

$$s' = \alpha(V)(1-s) - s/\tau$$

we want to find the average of $\alpha[V(t)]$ over one cycle, for then we can solve for the stationary state

$$0 = \langle \alpha[V(t)] \rangle (1-s) - s/\tau \tag{4}$$

for the average $\bar{s}$. Our conductance-based model is type I, so that the onset of rhythmic firing is via a saddle-node bifurcation. For synaptic gating variables of type I neurons $\langle \alpha(V) \rangle = K\sqrt{\bar{s}-a}$ [22]. A numerical evaluation of $\langle \alpha[V(t)] \rangle$ is very well approximated by $\sqrt{\bar{s}-0.002902}/5.1$. Using this expression in Eq. (4) and using a root finder, we obtain $\bar{s}=0.212$ which is very close to the value of 0.225 found by solving the boundary value problem and also close to the values for the simulation in Fig. 1(B1) with additive noise.

III. SIMPLIFIED MODEL

To understand the dynamic instability of the persistent state, we will introduce a simpler model for which we can better explore the nature of how persistence is lost. We have already noted that the biophysical model used in this paper is type I so that the onset of periodic solutions is via a saddle node on a circle. Near this bifurcation, the global dynamics is well approximated by the "theta" model which itself derives from a change of coordinates for the normal form of a saddle-node bifurcation of fixed points. Since we want to examine what happens with gap junctions, we will start with the normal form and make the appropriate change of variables.

If the gap junction coupling is weak, then the dynamics of two neurons near the bifurcation is equivalent to

$$x_j' = I_j + x_j^2 + g_{\text{gap}}(x_k - x_j) + \sigma \xi_j(t). \tag{5}$$

Here I_j are applied currents (including synaptic currents) and $\xi_j(t)$ is white noise. The change of variables to convert this model to the theta neuron is $x_j = \tan(\theta_j/2)$. Recalling that when there is a change of variable with a white noise process, we have to use Ito's formula [21], Eq. (5) becomes

$$\theta_j' = 1 - \cos(\theta_j) + (1+\cos\theta_j)\{I_j - \sigma^2/2 \sin\theta_j + g_{\text{gap}}[\tan(\theta_k/2) - \tan(\theta_j/2)] + \sigma\xi_j(t)\}. \tag{6}$$

One problem should now be apparent. When θ_k spikes, the right-hand side of the equation is singular. The half-angle formula for tangent is

$$\tan(\theta/2) = \frac{\sin\theta}{1+\cos\theta}.$$

The denominator vanishes only when the neuron spikes ($\theta=\pi$) and is otherwise positive. Thus, we simply add a small positive number to the denominator to obtain the nonsingular gap-junction model

$$q(\theta) = \frac{\sin(\theta)}{1+\cos\theta+\epsilon}.$$

With these preliminaries, our full model is

$$\theta_j' = 1 - \cos\theta_j + (1+\cos\theta_j)\{I + \sigma\xi_j(t) - \sigma^2/2 \sin\theta_j + g_{\text{syn}}\bar{s} + g_{\text{gap}}[\bar{q} - q(\theta_j)]\},$$

$$s_j' = \alpha_0(1-\cos\theta_j)^p - s_j/\tau,$$

$$\bar{s} = \frac{1}{N}\sum_k s_k,$$

$$\bar{q} = \frac{1}{N}\sum_k q(\theta_k).$$

We have chosen $\alpha_0=0.1$, $p=5$, $\epsilon=0.1$, $I=-0.05$. The amount of noise, σ varies between 0.05 and 0.35. The strength of the synapses, is usually 0.6 and the strength of the gap junctions is a parameter which we vary. The function $(1-\cos\theta)^p$ is nearly zero when the neuron is at rest ($\theta\approx 0$), but becomes large when the neuron fires ($\theta=\pi$). The choice of $p=5$ is arbitrary but chosen so that $s(t)$ has dynamics similar to those of the conductance-based model. The shape of $(1-\cos\theta)^5$ is similar to a Gaussian centered at π with a half width of about 1.

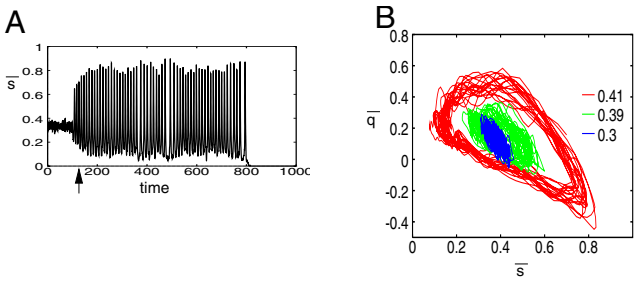

FIG. 3. (Color online) Behavior of the "theta" model for $N=200$ cells as g_{gap} increases. Noise level is $\sigma=0.05$, and rest of parameters are as in text. (A) For $t \geq 100$ $g_{\text{gap}}=0.43$. This destabilizes the steady state leading to large oscillations and then return to the resting state of no activity. (B) $\bar{q}$ and $\bar{s}$ for different strengths of the gap junctions.

Figure 3 shows that the simple model behaves in much the same way as the conductance-based model. Compare Fig. 1(B1) to Fig. 3(A). That is, strong gap junctions cause synchronization and then termination of persistent activity. For smaller gap junction strengths, the constant persistent state is unstable but there remains a persistent state which appears to oscillate as seen in Fig. 3(B). This figure shows the $(\bar{s},\bar{q})$ plane for three values g_{gap}.

IV. POPULATION DENSITY METHODS

To further analyze this model, we employ a population density method. Such methods are well known in neural

modeling and are often used to analyze asynchronous states in all-to-all connected networks [12,15,16,23–25]. Reference [6] applied weak coupling and population density methods to systems of quadratic integrate and fire models with noise to show the emergence of synchrony due to the gap junctions. However, here, we present an example of these methods applied to the interaction of *strong* synaptic and gap-junctional coupling in an excitable system. We let $P(\theta,t)d\theta$ denote the probability that a cell will have a phase in $(\theta,\theta+d\theta)$. The density (PDF), $P(\theta,t)$ satisfies the partial differential equation

$$\frac{\partial P(\theta,t)}{\partial t} = -\frac{\partial}{\partial \theta}[J(\theta,t)P(\theta,t)] + \frac{\sigma^2}{2}\frac{\partial^2[P(\theta,t)(1+\cos\theta)^2]}{\partial \theta^2}. \tag{7}$$

The term $J(\theta,t)$ is obtained from the deterministic part of the model

$$J(\theta,t) = 1-\cos\theta + (1+\cos\theta)\left[I + g_{\rm syn}\bar{s} + g_{\rm gap}[\bar{q}-q(\theta)] - \frac{\sigma^2}{2}\sin\theta\right]. \tag{8}$$

The quantities, $\bar{s},\bar{q}$ are the averages of the synapses and the gap function. $\bar{s}$ satisfies an ODE

$$\frac{d\bar{s}}{dt} = -\bar{s}/\tau + \int_0^{2\pi} P(\phi,t)\alpha(\phi)d\phi, \tag{9}$$

where $\alpha(\theta)=\alpha_0(1-\cos\theta)^p$. The gap junction term is defined by

$$\bar{q} = \int_0^{2\pi} P(\phi,t)q(\phi)d\phi. \tag{10}$$

$P(\theta,t)$ is 2π periodic and also normalized:

$$\int_0^{2\pi} P(\theta,t)d\theta = 1.$$

This is a nonlinear integropartial differential equation for which we have essentially no hope of solving analytically. Thus to study this, we will discretize the PDE and then use simulations to study it. We need to be a little bit careful—the choice of discretization should preserve the total probability. We divide $[0,2\pi)$ into m bins, $\theta_0=0$, $\theta_1=\Delta\theta,\ldots,\theta_{m-1}=(m-1)\Delta\theta$ where $\Delta\theta=2\pi/m$. We let $P_j(t)=P(\theta_j,t)$, $R_j(t)=J(\theta_j,t)P_j(t)$, and $W_j=\sigma^2P_j(1+\cos\theta_j)^2/2$. Then the discretization is

$$P_j' = \frac{R_{j-1}-R_{j+1}}{2\Delta\theta} + \frac{W_{j+1}-2W_j+W_{j-1}}{\Delta\theta^2}.$$

The integrals in Eqs. (9) and (10) are approximated as Riemann sums, e.g.,

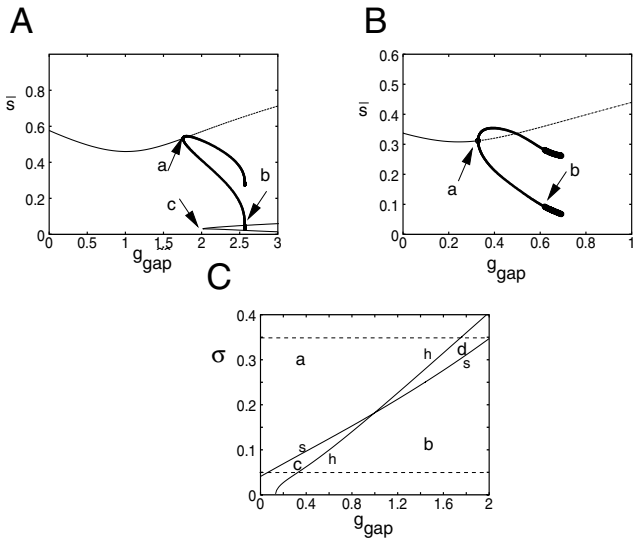

FIG. 4. Bifurcation diagram for the discretized version of Eq. (7) as the gap junction coupling $g_{\rm gap}$ varies with different levels of noise σ. (A) $\sigma=0.35$. The persistent state loses stability at a Hopf bifurcation (a). This leads to oscillatory persistent activity (filled circles) terminating on a homoclinic orbit (b). There is a stable state with very little activity for sufficiently strong gap junctions terminating at a saddle-node bifurcation (c). (B) $\sigma=0.05$. As in (A) the persistent state has a Hopf bifurcation (a). The resulting branch of periodic solutions (filled circles) loses stability at a period-doubling point (b). (C) Two parameter diagram showing curve of Hopf bifurcations of the persistent states (h) and the saddle-node curve for the quiescent state (s). Dashed lines correspond to noise values in (A), (B). See text for further discussion.

$$\bar{q} \approx \sum_{j=0}^{m-1} P_j q(\theta_j)\Delta\theta.$$

Normalization is achieved by replacing P_{m-1} by $(1-\Sigma_{k=0}^{m-2}P_k\Delta\theta)/\Delta\theta$. Thus, we eliminate the troublesome 0 eigenvalue associated with the normalization. This will enable us to use AUTO to perform a bifurcation analysis on the discretized system of ODEs. We used $m=50$ but checked some of the results with $m=100$.

Models similar to Eq. (7) have been studied by numerous authors; the most comprehensive analysis was done in Ref. [15]. References [16] and [16,17] used a numerical scheme to study similar models by writing $P(\theta,t)$ as a truncated Fourier series and solving the resulting set of ODEs for the coefficients. [24] use very sophisticated numerical techniques since they apply these methods to the leaky integrate-and-fire model which has a reset and so, leads to complicated nonlinear boundary conditions.

We find that the behavior of the PDF depends on the level of noise. Figure 4(A) shows a bifurcation diagram for the discretized version of Eq. (7) when the noise level is high, $\sigma=0.35$. As the gap junction strength increases the constant persistent activity state exists but at $g_{\rm gap}\approx 1.4$, it loses stability at a Hopf bifurcation [labeled (a)]. The result is a branch of stable periodic solutions. This branch appears to terminate at a homoclinic point [labeled (b) in Fig. 4(A)] when

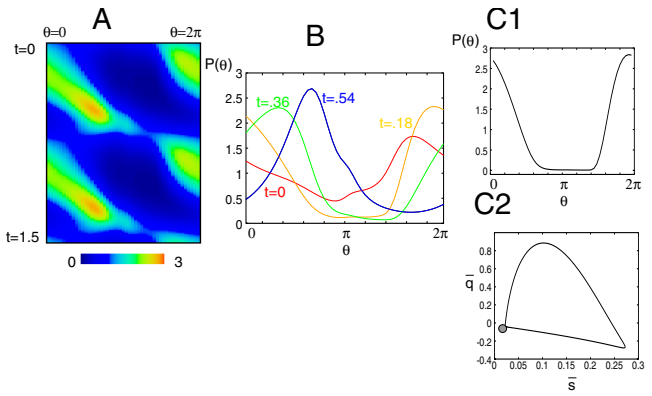

FIG. 5. (Color online) Global picture of the probability distribution in the periodic regime. $g_{syn}=0.6$, $\sigma=0.35$. (A) Space-time plot of $P_j(t)$ over two cycles for $g_{gap}=2.0$. (B) Spatial profiles at different times during the cycle. (C1) Stationary profile close to the homoclinic orbit ($g_{gap}=2.56515311$); (C2) projection of the homoclinic orbit in the $(\bar{s},\bar{q})$ plane.

$g_{gap}\approx 2.0$. For sufficiently strong gap junctions, there is a state of low activity (quiescent) where $\bar{s}$ is essentially 0. As the gap junctions decrease, this quiescent state terminates at a saddle-node bifurcation [labeled (c)]. The noise is sufficiently high so that the quiescent state ($\bar{s}\approx 0$) does not exist without gap junctions. That is, fluctuations due to noise are sufficient to push the network into the asynchronous persistent state. There is a regime of bistability between the periodically varying state and the quiescent state [between the points labeled b and c in Fig. 4(A)]. For a finite size system, it is possible to jump from the stable periodic system to the quiescent system, thus even if $g_{gap}<2$, it is possible to spontaneously terminate persistent activity.

At low values of noise (e.g., 0.025), the situation is quite different [Fig. 4(B)]. First, the quiescent state exists for all values of g_{gap} (not shown in the figure as it is indistinguishable from the $\bar{s}=0$ axis). As in the high noise case, the constant persistent state loses stability at a Hopf bifurcation at $g_{gap}\approx 0.3$. The branch of periodic solutions emanating from the equilibrium state loses stability through a period doubling bifurcation [Fig. 4(Bb)] at $g_{gap}\approx 0.6$. Figure 4(C) summarizes the local equilibrium behavior in the noise (σ) gap junction (g_{gap}) plane. There are two lines representing the curve of Hopf bifurcation points for the persistent state (labeled "h") and the curve of saddle-node points for the existence of the quiescent state (labeled "s"). Note that these curves describe the critical curves for two different fixed points. Thus, their intersection does not correspond to a local codimension two bifurcation. In the regions labeled (a),(c), the persistent state exists and is stable. In the regions labeled (b),(d), the quiescent state exists and is stable. In region (c), the persistent and quiescent states coexist.

Figure 5 provides a picture of the global dynamics of the PDF in the periodic persistent regime. Here, oscillations occur in the $P(\theta,t)$ with a period of about 0.75. Figure 5(B) shows the shapes of the PDF at different times. Similar behavior is found in the low noise case, but the variations in the probabilities are much more extreme. In the high-noise case, as the gap junctions strength increases, the periodic solutions

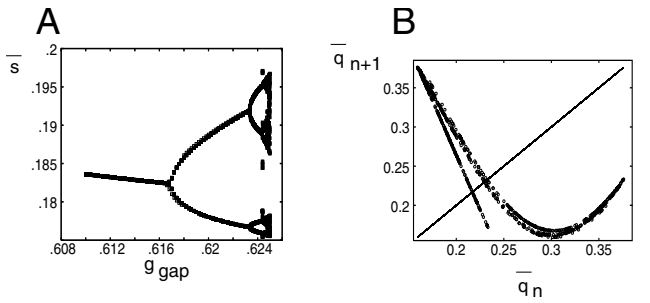

FIG. 6. Chaotic behavior with low noise ($\sigma=0.05$) as g_{gap} varies. (A) Value of $\bar{s}$ each time $\bar{q}$ crosses 0 from below after a transient of 200 for 300 time units. Period doubling sequence is clearly evident. (B) Apparent chaos when $g_{gap}=0.625$. Plot of $\bar{q}$ when $\bar{s}$ crosses 0.2 from below.

appear to merge with a steady state forming a homoclinic loop [Fig. 4(A)]. Figure 5(C) shows the numerical solution near the homoclinic orbit. The stationary probability distribution shown in Fig. 5(C1) has a single positive eigenvalue with a one-dimensional unstable manifold which forms the homoclinic orbit. The projection of this orbit is shown in Fig. 5(C2). We have doubled the grid size and find that this PDF still has only one positive eigenvalue.

In the low noise case, the periodic persistent state loses stability at a period-doubling bifurcation. We zoom in on this behavior in Fig. 6(A). Since $\bar{q}$ reliably passes through 0 on every cycle, we plot $\bar{s}$ at each time when $\bar{q}$ increases through 0. For a very small range of g_{gap} there is a period doubling route to chaos. The period 4 and 8 bifurcations can be easily picked out, but the higher period bifurcations are less discernible. Figure 6(B) shows the dynamics when $g_{gap}=0.625$. Each time $\bar{s}$ increases through 0.2, we plot the value of $\bar{q}$. This plot shows the $n+1$ crossing against the n crossing for several thousand points. The plot suggests that the dynamics is nearly captured by a one-dimensional unimodal map. As g_{gap} gets a bit beyond 0.625, the persistent state ceases to stably exist and the only behavior is the quiescent state.

V. THE CONDUCTANCE-BASED MODEL REVISITED

While the complex behavior in the low noise case would likely be washed out in the conductance-based model with a finite number of neurons, the higher noise behavior would seem to be more robust. In particular, if the simple model is a reasonable caricature of the full conductance-based system, we should see evidence for the destabilization of the constant persistent state and the termination of the oscillations via a homoclinic bifurcation as in Figs. 4(A), and 5(C1), 5(C2). Indeed, Fig. 1(B) suggests exactly this. There are growing oscillations whose period appears to increase with amplitude. The "kink" in the phase-plane trajectory [Fig. 1(B2)] near the point $(0.05,-60)$ is also suggestive of a possible saddle-point type dynamics which would be associated with a homoclinic orbit. In order to investigate this possibility more thoroughly, we solve the full stochastic model (1), while varying g_{gap} and tracking the interval between crossings of

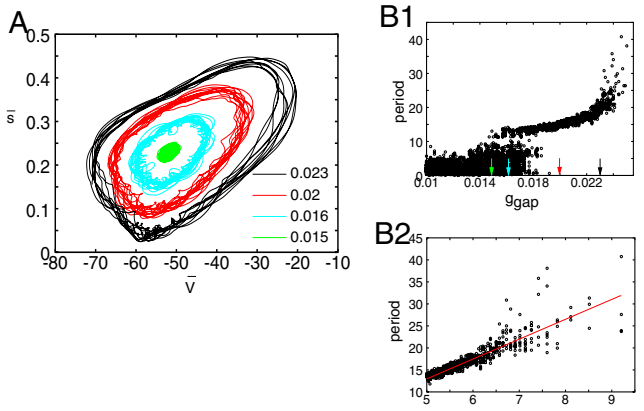

FIG. 7. (Color online) Simulation of the conductance-based model as g_{gap} varies. (A) Phase-plane showing noisy limit cycles as g_{gap} increases. (B1) Interval between crossings of $\bar{s}=0.226$ as g_{gap} changes. Between 0.014 and 0.015, the persistent state appears to lose stability and gives rise to a robust periodic variation of $\bar{s}$ around its steady state. The period becomes large and the limit cycle disappears at about $g_{gap}=0.0245$. (B2) Plot of period versus $-\ln(0.0245-g_{gap})$ is close to linear.

$\bar{s}=0.226$ which is close to the steady state for persistent activity. Figure 7(A) shows a series of noisy limit cycles generated by the conductance-based model for several values of g_{gap}. The average potential of the network and the average synaptic strength are plotted in the plane. For $g_{gap}<0.015$, the persistent state seems to exist and is stable. For g_{gap} slightly larger, this state loses stability and a small amplitude oscillation emerges just as in the theta model [Fig. 4(A)]. The oscillation grows in amplitude as g_{gap} increases. At $g_{gap}=0.023$, the limit cycle shows a clear "kink" suggesting that it arises from a homoclinic bifurcation. Figure 7(B1) shows intervals between crossing of $\bar{s}=0.226$ as g_{gap} increases. For $g_{gap}<0.015$, the crossing times are random but for $g_{gap}>0.015$ order emerges and a true time scale becomes apparent. It appears that the crossing times are growing to infinity. At a homoclinic bifurcation, we expect that the periodgrows as

$$T \sim -K \ln|p-p^*|,$$

where p is a parameter and p^* is the point at which there is a homoclinic bifurcation. Figure 7(B2) shows a plot of the period as a function of $-\ln(0.0245-g_{gap})$. We plot the best least-squares fit of the line as well. Even though there are only 100 neurons in the network and there is substantial noise, these results strongly suggest the existence of a homoclinic bifurcation in the full conductance-based system.

In both the high and low noise cases of the theta model, there is a constant persistent state which seems to lose stability via a Hopf bifurcation. There is a suggestion of this bifurcation in the conductance-based model as well. We now consider an approximation which allows us to estimate the value of the critical gap junction strength which leads to a loss of stability of the constant persistent state. The simulations and analysis demonstrate that the mechanism appears to be due to the local synchronization of the oscillators, thus we will use a weak-coupling approximation to analyze the stability of the asynchronous state. The idea is as follows. We write $s_j(t)=\bar{s}+y_j(t)$ where $\bar{s}$ is the tonic component of the persistent activity. For example in Fig. 1, $\bar{s}\approx 0.23$. We assume that the gap junctions are weak. Thus, we can write Eq. (1) as

$$C\frac{dV_j}{dt} = -I_{ion} - g_{syn}\bar{s}V_j - \sum_k [(g_{syn}/N)y_k V_j + (g_{gap}/N)(V_j - V_k)] + \sigma\xi_j(t).$$

The variables y_j satisfy the differential equation

$$\frac{dy_j}{dt} = 2(1-\bar{s}-y_j)/[1+\exp(-V_j/4)] - (\bar{s}+y_j)/3.$$

Coupling between neurons is only via the terms in the summation. In absence of these terms, each cell will fire periodically due to the tonic drive from $\bar{s}$. We regard this as a (noisy) system of weakly coupled oscillators. With small noise, this conductance-based system can be reduced to a system of coupled phase models [26]:

$$\frac{d\phi_j}{dt} = 1 + \frac{1}{N}\sum_k [g_{syn}H_{syn}(\phi_k-\phi_j) + g_{gap}H_{gap}(\phi_k-\phi_j)] + \sigma\xi_j(t). \quad (11)$$

The periodic functions H_{syn}, H_{gap} are obtained from averaging:

$$H_{syn}(\phi) = -\frac{1}{P}\int_0^P V^*(t)V(t)y(t+\phi)dt,$$

$$H_{gap}(\phi) = \frac{1}{P}\int_0^P V^*(t)[V(t+\phi)-V(t)]dt,$$

where $V(t), y(t)$ are the P-periodic solutions to the uncoupled oscillator and $V^*(t)$ is the periodic solution to the linear adjoint equation (see Ref. [27]). These functions are easily computed numerically using the package XPPAUT [28]. The analysis of Eq. (11) follows the work of Ref. [29], wherein the stability of the asynchronous state (phase distribution is uniform) is analyzed. Without going into details, it is easy to show that the asynchronous state is stable only if

$$\nu_m = -\sigma^2 m^2/2 + m[g_{syn}a_m + g_{gap}b_m] < 0$$

for all m. (Reference [6] obtain a similar result.) The parameters, a_m, b_m are the sine coefficients of the Fourier expansion of the functions $H_{syn}(\phi)$ and $H_{gap}(\phi)$, respectively. With noise, for m large, $\nu_m<0$ so that practically speaking, only the lower order harmonics matter. We compute these coefficients for the conductance-based model and find that the coefficients for $m=1$ are almost an order of magnitude larger than those for $m>1$ and that $a_1=-0.106$ and $b_1=1.18$. Since $g_{syn}=0.15$, we see that the minimum gap junction strength to destabilize the constant persistent state is roughly $g^*_{gap}\approx 0.0135$ (when noise is zero). Examination of Fig. 7(B1) indicates that the onset of instability in the presence of small noise is at $g_{gap}\approx 0.015$ which is close to our estimate. Similar estimates can be applied to the theta model to deter-

mine the coupling strength for the synchronizing instability. We remark that the critical gap function strength is a monotonically increasing function of the noise and furthermore a close examination of Fig. 4(C) reveals that for low noise, the critical gap strength depends quadratically on σ as predicted from the formula for ν_m.

VI. DISCUSSION

Gap junctions are rarely seen in recurrent excitatory networks yet they are ubiquitous in inhibitory networks. We suggest that the main role for gap junctions is to encourage synchronization during rhythmic behavior. Synchrony, because it leads to a "shared" refractory period between neurons can lead to the extinction of persistent activity. While there are situations in which gap junctions do not produce synchrony [5,6], in most biophysical models for cortical neurons, they encourage synchrony.

It is easy to imagine situations in which gap junctions could alone produce a persistent state if the coupling is sparse. Indeed, spiral waves and irregular activity are known to occur in two-dimensional media with local coupling. Reference [30] described a spatially distributed sparsely coupled network of excitable cells and found spontaneous oscillatory activity. However, crucial to the generation of this activity was the existence of cells that could spontaneously spike. For example, a large amount of noise could cause a neuron to spontaneously fire. The coupling between cells would cause the spiking to propagate and result in a population spike. The refractory period of the cells would prevent another spike from occurring until some time has elapsed. With enough cells and with enough connectivity, then the spiking would be regular. This is not like the persistent activity seen in synaptically coupled networks where the coupling encourages asynchrony. The Lewis-Rinzel model produces nearly synchronous oscillations for exactly the reason that gap junctions destroy asynchrony; in both cases the role of gap junctions is to cause neurons to fire in concert.

Dynamic destabilization of persistent states has been considered by numerous authors. The methods of Refs. [16,17] are the closest to those used here. They looked at networks of excitatory and inhibitory cells using a model similar to, but not the same as the theta model. References [12,15] analyzed the quadratic integrate-and-fire model with finite spike and reset. They showed that the persistent state could undergo a synchronizing instability as the degree of inhibitory coupling changed. Depending on the time constant of recurrent excitation and inhibition, the persistent state could begin to oscillate much as in our case or, for fast time constants, disappear. Our contribution has shown that similar behavior occurs with gap junctional coupling. The present results require that the synaptic coupling be sufficiently strong to produce a persistent state since weak synaptic coupling will not be enough to overcome the attraction of the stable rest state. We have not yet explored whether sparse coupling will enhance or hurt the existence of the persistent state. Clearly, one effect of sparseness in the synaptic coupling is to introduce heterogeneity which will in turn make the asynchronous state more likely. We have used the biophysical and simplified models to suggest that a possible reason for the lack of gap junctions in recurrent excitatory networks is that they disrupt persistent states which may be necessary for working memory.

In the case of synaptic coupling, it is possible to develop simplified mean field models which can explain some aspects of the instability of the persistent state. Reference [22] showed this in a population of conductance-based neurons when the synapses are slow and Ref. [15] found a similar phenomena also when the synapses were slow. For example, in a purely excitatory network, the total synaptic activity (without gap junctions) is well approximated *even dynamically* by the equation

$$\tau_{\rm syn}\frac{d\bar{s}}{dt} = -\bar{s} + \gamma_0 F(\bar{s})(1-\bar{s}),$$

where $F(s)$ is the firing rate of an individual neuron as a function of the synaptic gating variable. This is just a dynamic version of Eq. (4). One open question is whether there is a simplified mean field theory for networks which involve gap junctional coupling.

ACKNOWLEDGMENTS

The author was supported in part by NIMH and NSF.

APPENDIX A: MODEL KINETICS

Parameters for the conductances, etc are $g_L=0.0092$, $E_L=-61.52$, $g_{Na}=35$, $E_{Na}=45$, $g_K=25$, $E_K=-95$, $E_{\rm syn}=0$, $g_{\rm syn}=0.15$, $C=0.29$. The channel kinetics are

$$a_m(v) = 0.091(v+38)/\{1-\exp[-(v+38)/5]\},$$

$$b_m(v) = -0.062(v+38)/\{1-\exp[(v+38)/5]\},$$

$$a_h(v) = 0.016\exp[(-55-v)/15],$$

$$b_h(v) = 2.07/\{1+\exp[(17-v)/21]\},$$

$$a_n(v) = 0.01(-45-v)/\{\exp[(-45-v)/5]-1\},$$

$$b_n(v) = 0.17\exp[(-50-v)/40],$$

$$\alpha(v) = 1/[1+\exp(-v/4)].$$

The synapse satisfies

$$s' = \alpha(V)(1-s) - s/3.$$

APPENDIX B: BOUNDARY VALUE PROBLEM

We rescale time, $t=Pt'$ with P, the unknown period, so that the single cell model can be written as

$$V' = PF(V,m,n,h,\bar{s},\bar{V}),$$

$$m' = P[a_m(V)(1-m) - b_m(V)m],$$

$$h' = P[a_h(V)(1-h) - b_h(V)h],$$

$$n' = P[a_n(V)(1-n) - b_n(V)n],$$

$$s' = P[\alpha(V)(1-s) - s/\tau],$$

$$y' = s,$$

$$z' = V.$$

We must solve this set of equations subject to

$$V(0) = 0,\ V(1) = 0,\ m(0) = m(1),\ h(0) = h(1),\ n(0) = n(1),\ s(0) = s(1),\ y(0) = 0,\ y(1) = \bar{s},\ z(0) = 0,\ z(1) = \bar{V}.$$

We have seven differential equations with ten boundary conditions. But the period of the limit cycle P, the mean value of the synapse $\bar{s}$, and the mean voltage $\bar{V}$ are free parameters. So this gives us the appropriate number of unknowns. We solve the BVP initially by using the full simulations to get a good guess for $P, \bar{s}, \bar{V}$. We use shooting to obtain one good solution to the BVP. Then we use AUTO to continue the solution as parameters change.

[1] X. J. Wang, J. Neurosci. **19**, 9587 (1999).
[2] A. Compte, N. Brunel, P. S. Goldman-Rakic, and X. J. Wang, Cereb. Cortex **10**, 910 (2000).
[3] T. I. Netoff and S. J. Schiff, J. Neurosci. **22**, 7297 (2002).
[4] D. Golomb, A. Shedmi, R. Curtu, and G. B. Ermentrout, J. Neurophysiol. **95**, 1049 (2006).
[5] C. C. Chow and N. Kopell, Neural Comput. **12**, 1643 (2000).
[6] B. Pfeuty, G. Mato, D. Golomb, and D. Hansel, J. Neurosci. **23**, 6280 (2003).
[7] B. Pfeuty, G. Mato, D. Golomb, and D. Hansel, Neural Comput. **17**, 633 (2005).
[8] B. Ermentrout, J. W. Wang, J. Flores, and A. Gelperin, J. Comput. Neurosci. **17**, 365 (2004).
[9] T. J. Lewis and J. Rinzel, J. Comput. Neurosci. **14**, 283 (2003).
[10] R. D. Traub, H. Michelson-Law, A. E. Bibbig, E. H. Buhl, and M. A. Whittington, Adv. Exp. Med. Biol. **548**, 110 (2004).
[11] S. W. Hughes, M. Lorincz, D. W. Cope, K. L. Blethyn, K. A. Kekesi, H. R. Parri, G. Juhasz, and V. Crunelli, Neuron **42**, 253 (2004).
[12] D. Hansel and G. Mato, Phys. Rev. Lett. **86**, 4175 (2001).
[13] B. S. Gutkin, C. R. Laing, C. L. Colby, C. C. Chow, and G. B. Ermentrout, J. Comput. Neurosci. **11**, 121 (2001).
[14] C. R. Laing and C. C. Chow, Neural Comput. **13**, 1473 (2001).
[15] D. Hansel and G. Mato, Neural Comput. **15**, 1 (2003).
[16] T. Kanamaru and M. Sekine, Phys. Rev. E **67**, 031916 (2003).
[17] T. Kanamaru, Neural Comput. **18**, 1111 (2006).
[18] J. Huguenard, D. A. McCormick, and G. M. Shepherd, *Electrophysiology of the Neuron: An Interactive Tutorial/Book and Disk* (Oxford University Press, Oxford, 1994).
[19] G.-B. Ermentrout and N. Kopell, SIAM J. Appl. Math. **46**, 233 (1986).
[20] B. Ermentrout, Neural Comput. **8**, 979 (1996).
[21] B. Lindner, A. Longtin, and A. Bulsara, Neural Comput. **15**, 1760 (2003).
[22] B. Ermentrout, Neural Comput. **6**, 679 (1994).
[23] A. Omurtag, E. Kaplan, B. Knight, and L. Sirovich, Network **11**, 247 (2000).
[24] D. Cai, L. Tao, M. Shelley, and D. W. McLaughlin, Proc. Natl. Acad. Sci. U.S.A. **101**, 7757 (2004).
[25] L. Sirovich, A. Omurtag, and K. Lubliner, Network **17**, 3 (2006).
[26] Y. Kuramoto *Chemical Oscillations, Waves, and Turbulence* (Springer, New York, 1984).
[27] G. B. Ermentrout and N. Kopell, SIAM J. Appl. Math. **15**, 215 (1984).
[28] G. B. Ermentrout, *Simulating, Analyzing, and Animating Dynamical Systems* (SIAM, Philadelphia, 2002).
[29] S. H. Strogatz, Physica D **143**, 1 (2000).
[30] T. J. Lewis and J. Rinzel, Network **11**, 299 (2000).